15.6 A NUMERICAL MODELING STUDY OF THE MICROPHYSICAL PROCESSES LEADING TO TROPICAL CYCLOGENESIS UNDER DIFFERENT ENVIRONMENTAL CONDITIONS

Andrew B. Penny* and Elizabeth A. Ritchie
Department of Atmospheric Sciences, University of Arizona

1. INTRODUCTION

Although great strides have been made towards increasing our understanding of tropical cyclogenesis from both observational and modeling perspectives, there is still a lack of consensus within the scientific community as to how tropical disturbances are able to develop a near-surface vortex and warm-core characteristics, and transform into a self-sustaining tropical cyclone.

Several theories have proposed that the presence of a midlevel convective vortex (MCV) is an important precursor for tropical cyclogenesis (Chen and Frank 1993; Fritsch et al. 1994; Ritchie and Holland 1997). It has been hypothesized that a MCV might help "spin-up" a disturbance's near-surface circulation through the direct transport of positive cyclonic relative vorticity down near the surface (Bister and Emanuel 1997), or as a result of vortex merger processes, which act to increase the penetration depth of the midlevel PV anomaly associated with a MCV (Ritchie and Holland 1997, Simpson et al. 1997).

However, more recent modeling studies suggest a lower-tropospheric, convectively driven route to tropical cyclogenesis. The modeling studies of Hendricks et al. (2004) and Montgomery et al. (2006) indicate that deep convection possessing high values of cyclonic relative vorticity, or "vortical hot towers" (VHTs), are the essential building blocks for tropical cyclone formation. The modeling studies by Tory et al. (2006a,2006b,2007) and Kieu and Zhang (2008,2009) reveal that MCVs may play a role in some tropical cyclogenesis cases, but that the development of a lower-tropospheric vortex can be attributed almost exclusively to low-level convective processes.

Although numerical modeling studies have focused on tropical cyclogenesis from an idealized and case study perspective, to date, a comparative study involving two real-life case studies is still lacking. This modeling study attempts to address this need by focusing on two Western North Pacific tropical cyclones, Typhoons Ketsana (2003) and Mawar (2005), which formed within contrasting environments and exhibited notable differences, and compares the mesoscale processes of the modeled storms prior to and during tropical cyclogenesis. Although the storms were significantly different in size and structure, the model simulations suggest they shared a similar vorticity evolution in which stratiform and convective processes were important. The remainder of this paper is divided as follows: part two describes the model setup used to conduct this study and provides a brief comparison of the model solution with observations, part three discusses the results, and part four concludes.

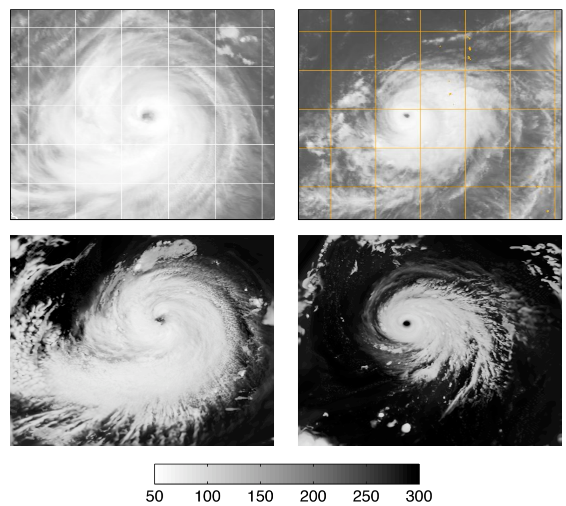

Figure 1: Infrared satellite image of Typhoon Ketsana (top left) at 19Z October 21, 2003 and Typhoon Mawar (top right) at 23Z August 21, 2005 shown for comparison with model-derived outgoing longwave radiation (W m^{-2}) at 96 hours for the Typhoon Ketsana simulation (bottom left) and Typhoon Mawar simulation (bottom right).

2. METHODOLOGY

2.1 Model configuration

Two numerical simulations of tropical cyclogenesis were conducted using the Advanced Weather Research and Forecasting (WRF-ARW) model version 3.0 developed by the National Center for Atmospheric Research (NCAR). Each simulation consisted of three nested domains with resolutions of 15-, 5-, and 1.67-km with 33 vertical model levels. The finest resolution grid (1.67-km grid spacing) consisted of 700 x 700 grid points in each simulation. The two inner domains were allowed to follow the developing storms using a vortex-tracking

**Corresponding author address:* Andrew B. Penny, University of Arizona, Department of Atmospheric Sciences, Tucson, AZ, 85721-0081; email: penny@atmo.arizona.edu.

algorithm that locates the vortex based on a local minimum of the 500 mb height field within a particular search radius.

Microphysical processes were represented by the WRF Single-Moment 6-class (WSM6) scheme, which allows for snow, ice, and graupel effects. The Kain-Fritcsh cumulus parameterization scheme was implemented for the coarsest domain (15-km grid spacing), but convection was explicitly represented (no cumulus scheme) for the two nested domains. Boundary layer processes were parameterized using the Yonsei University (YSU) planetary boundary layer scheme. Each simulation was conducted using 6-hourly National Center for Environmental Prediction (NCEP) Final Analysis (FNL) data.

The Typhoon Ketsana simulation was integrated from 00Z October 18 to 00Z October 25, 2003 for a total of 168 hours, and the Typhoon Mawar simulation extended from 00Z August 18 to 00Z August 26, 2005 for a total of 192 hours.

2.2 Overview comparison of observations and model simulations

Typhoons Ketsana (2003) and Mawar (2005) formed within vastly different environments. Ketsana developed within the monsoon trough east of the Philippines, and strengthened to a maximum intensity of 64 m s^{-1} by 12Z October 21, 2003 (JTWC 2003). Typhoon Mawar formed further to the north, away from the favorable influence of the monsoon trough, but due to weak vertical wind shear, Mawar developed into an intense tropical cyclone with a compact wind field, reaching a peak intensity of 65 m s^{-1} by 18Z August 21, 2005 (JTWC 2005).

The simulations of Typhoon Ketsana and Typhoon Mawar did a reasonable job at representing the two Western North Pacific storms, although notable differences did exist, especially in the time of development for Ketsana. Figure 1 compares the structure of the simulations using model-derived outgoing longwave radiation with infrared satellite observations, and reveals that the structure of the modeled storms agrees closely with what was observed; Ketsana was a very large storm and exhibited a highly asymmetric structure in comparison to Mawar.

3. RESULTS AND DISCUSSION

Although the modeled storms were different in size and structure, the simulations of Ketsana and Mawar shared a similar development process. Figure 2, which compares minimum sea-level pressure and azimuthally averaged 850 mb wind speed at the radius of maximum winds, reveals that each modeled storm underwent three similar stages of development. The first phase (0-36 hours in both simulations) was characterized by bursts of deep convection, and only a small decline in minimum sea-level pressure was noted during this time. The second phase encompassed tropical cyclogenesis (~36-72 hours), and was marked by a slight increase in the rate of pressure decline. During the third phase, which extended from 72-120 hours in the Ketsana simulation and from 72-96 hours in the Mawar simulation, both simulations experienced rapid intensification.

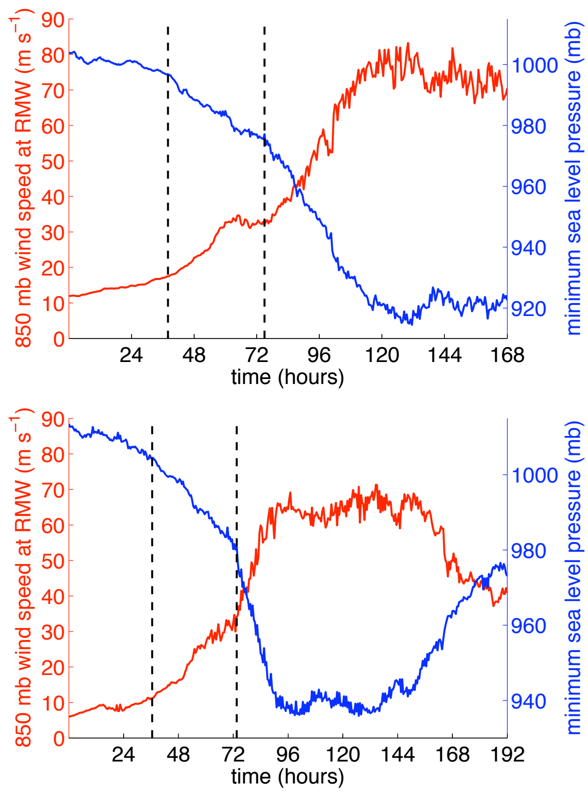

Figure 2: Minimum sea-level pressure (mb) and azimuthally averaged 850 mb wind speed (m s^{-1}) at the radius of maximum winds for the Typhoon Ketsana simulation (top) and Typhoon Mawar simulation (bottom). Vertical dashed lines separate the three phases of development. The first phase of development was marked by deep convective bursts, the second phase encompassed tropical cyclogenesis, and the third phase was characterized by the rapid intensification of each storm.

3.1 Pre-genesis

In both the Ketsana and Mawar simulations, periods of deep convection occurred prior to genesis. Figure 3, which compares azimuthally averaged cloud-top temperature, reveals that the Ketsana simulation exhibited a period of deep convection between 24 and 36 hours, as the 0-100 km average cloud-top temperature dropped to -70°C during this time period (asterisks in Figure 3 and other figures denote the time of pre-genesis convective bursts in each simulation). For Mawar, at least three distinct periods of deep convection occurred before the storm experienced genesis, however, the averaged cloud-top temperature during Mawar's pre-genesis convective bursts was much warmer (-55°C) than it was for the deep convection prior to genesis in the Ketsana simulation. This pattern of convective bursts prior to genesis was observed in the infrared satellite imagery study by Zehr (1992) and is suggested to be an important stage in the tropical cyclogenesis process.

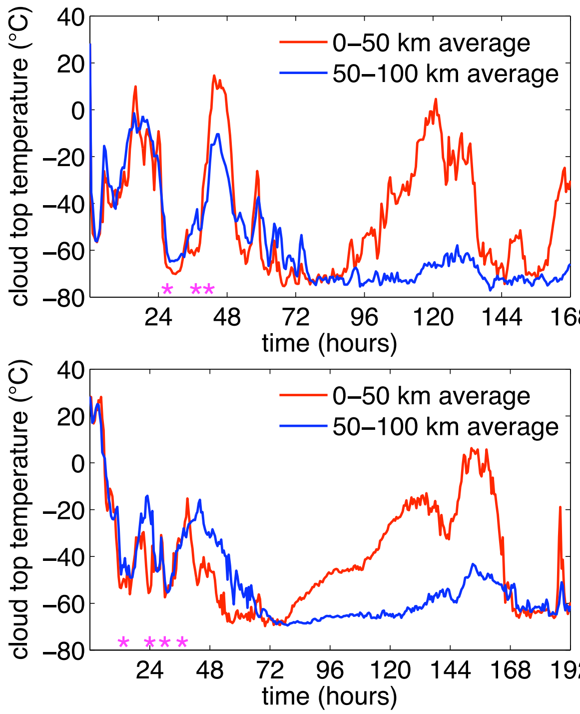

Figure 3: Azimuthally averaged (0-50 km radius and 50-100 km radius) cloud-top temperature (°C) for the Typhoon Ketsana simulation (top) and Typhoon Mawar simulation (bottom). Asterisks denote the time of pre-genesis convective bursts in each simulation.

Azimuthally averaged vertical velocity (0-50 km radius), which is shown in Figure 4, reveals periods of enhanced updrafts prior to genesis corresponding to the drop in cloud-top temperature associated with the pre-genesis convective bursts shown in Figure 3. The updraft structure in the Mawar simulation appears to have been better organized vertically than in the Ketsana simulation, as updrafts extended down from the upper-troposphere well into the low-levels. The disorganized structure of vertical velocity exhibited in the Ketsana simulation might have been due to strong vertical wind shear that was affecting the disturbance during this time (not shown).

Midlevel warming due to the convective bursts was evident in both simulations (not shown), and this caused a sharpening of the vertical temperature gradient. Evaporative cooling below the cloud deck in conjunction with the diabatic heating helped to increase midlevel potential vorticity (PV) in both simulations, which is shown in Figure 5. The bulk of the rise in midlevel PV in the Mawar simulation near 24 hours appears to have occurred between convective bursts, and this suggests that stratiform processes were acting to enhance PV during this time.

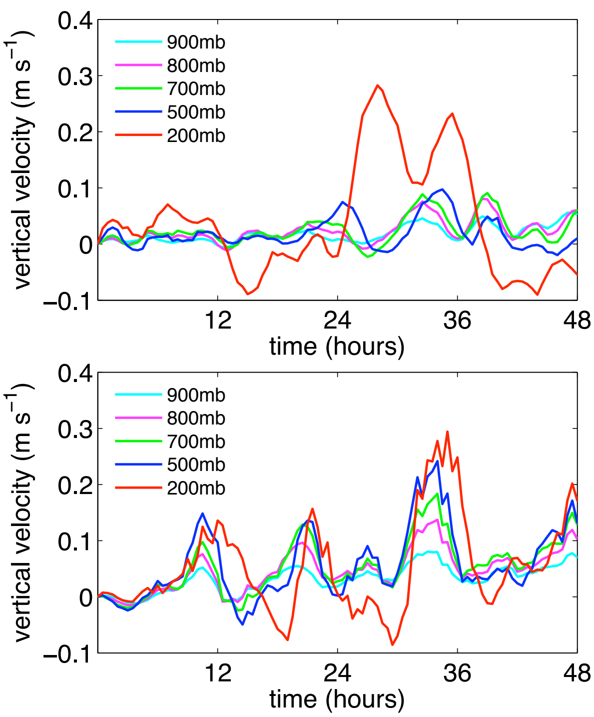

Figure 4: Azimuthally averaged (0-50 km radius) vertical velocity (m s^{-1}) for the Typhoon Ketsana simulation (top) and Typhoon Mawar simulation (bottom). The data were smoothed using a 2.5-hour running mean.

Figure 6, which compares relative vorticity, appears to indicate that relative vorticity increased from the "bottom-up" in the Ketsana simulation and from the "top-down" for Mawar. However, an analysis of the relative vorticity anomaly (Figure 7), calculated by differencing the initial azimuthally averaged relative vorticity profile from the average at later times, reveals a more complicated vorticity evolution for Ketsana. Although the relative vorticity appears to have increased first from within the lower-troposphere, where there was an abundance of positive cyclonic relative vorticity due to the monsoon trough environment, there was a region in the midlevels where the relative vorticity was also increasing.

Understanding the role that the increase in PV and relative vorticity within the midlevels had on the development of each storm, however, is difficult to pinpoint. The vertical flux convergence of relative vorticity (not shown) fails to show evidence of a downward transport of relative vorticity from the midlevels towards the surface. If present, this would have supported the theory proposed by Bister and

Emanuel (1997) that suggests that the downward flux of relative vorticity might occur through precipitative downdrafts. Instead, relative vorticity budgets, calculated on isobaric coordinates (not shown), reveal that once the lower-tropospheric wind profile became sufficiently convergent through a significant depth, the increase in low-level relative vorticity was dominated by the convergence of relative vorticity in the lower-troposphere, indicative of low-level convective processes.

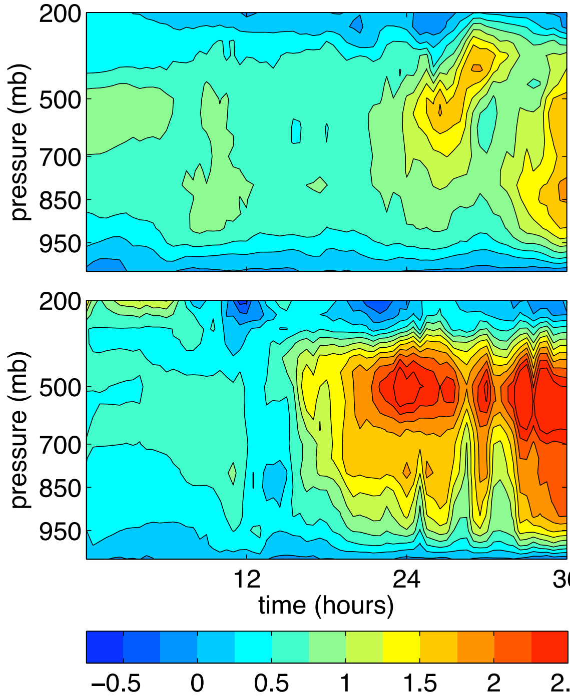

Figure 5: Azimuthally averaged (0-50 km radius) potential vorticity (PVU) for the Typhoon Ketsana simulation (top) and Typhoon Mawar simulation (bottom).

However, it is hypothesized that before the low-level convective processes became dominant, the presence of a midlevel PV anomaly played an important role in the development of each storm. As other studies have suggested (Ritchie and Holland 1997; Davis et al. 2009), the presence of a MCV might have helped organize the large-scale, low-level convergent wind profile that helped drive deep convection and increase lower-tropospheric relative vorticity. In addition, once convectively-driven processes became the primary mechanism for low-level relative vorticity enhancement, the presence of a midlevel PV feature, and its associated rise in midlevel inertial stability (not shown), allowed for a more efficient development of a positive temperature anomaly within the mid-troposphere of each storm. As inertial stability increases, there is increased resistance to radial displacements within the flow. This helps to “stiffen” the vortex and increases the efficiency by which local warming occurs through convection in a similar manner to that proposed by Schubert and Hack (1982), allowing for a more rapid development of a storm's warm core.

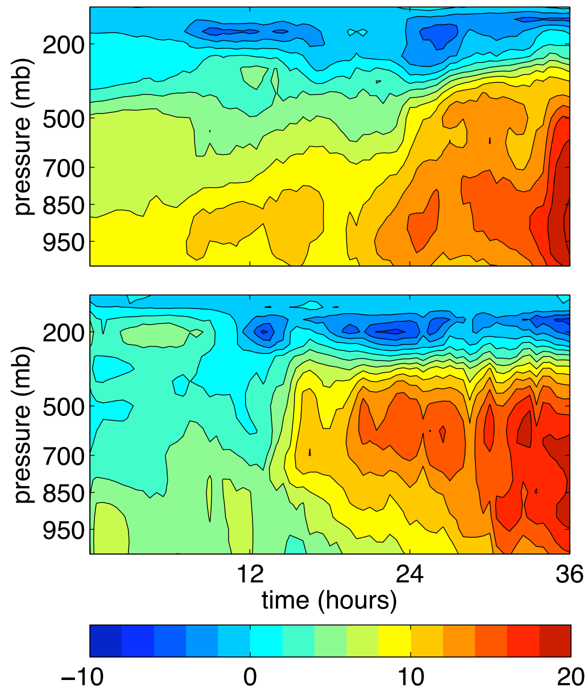

Figure 6: Azimuthally averaged (0-100 km radius) relative vorticity ($x10^{-5}$ s^{-1}) for the Typhoon Ketsana simulation (top) and Typhoon Mawar simulation (bottom).

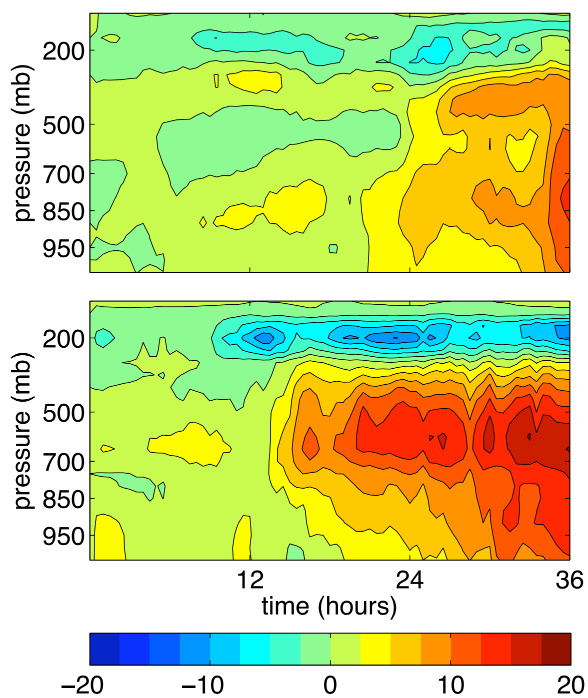

Figure 7: Azimuthally averaged (0-100 km radius) relative vorticity anomaly ($x10^{-5}$ s^{-1}) for the Typhoon Ketsana simulation (top) and Typhoon Mawar simulation (bottom).

Bursts of deep convection also appear to have been instrumental in the formation of near-surface negative temperature anomalies, which formed as a result of evaporative cooling. Figure 8, which shows the azimuthally averaged 975 mb temperature anomaly at various radii, calculated by differencing the temperature within the inner core of the disturbance from the 200-500 km azimuthal average of temperature, reveals that an inner-core cold pool formed in each simulation during the pre-genesis convective bursts. The presence of a cold pool appears to have helped sustain deep convection as the strongest updrafts in each simulation were located above significantly negative temperature anomalies (not shown). The near-surface cold pools acted as a lifting mechanism for converging high-equivalent potential temperature (θ_e) air.

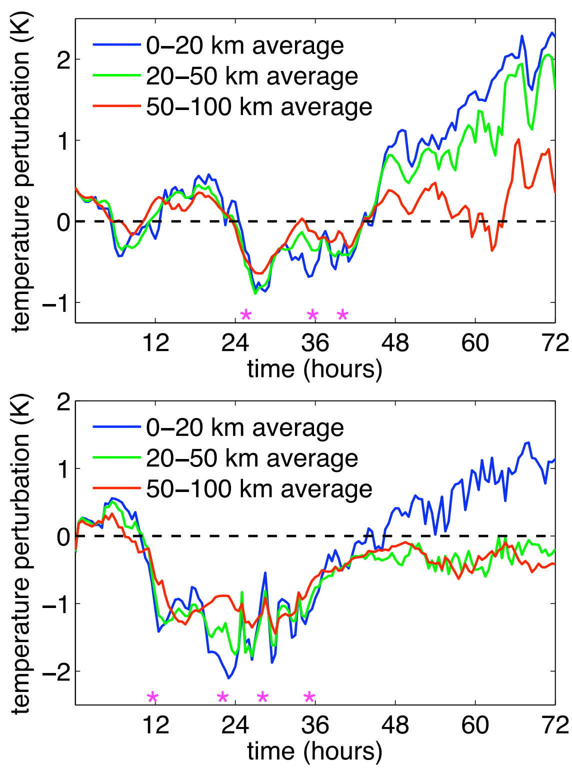

Figure 8: Azimuthally averaged (0-20 km, 20-50 km, and 50-100 km radius) 975 mb temperature anomaly (K) for the Typhoon Ketsana simulation (top) and Typhoon Mawar simulation (bottom). Asterisks denote the time of pre-genesis convective bursts in each simulation.

It is also worth noting that at the time of the convective bursts prior to genesis, θ_e decreased or remained nearly steady in the lower-troposphere, but increased in the midlevels (Figure 9). The transport of high-θ_e air into the midlevels via deep convection occurred simultaneously with enhanced surface fluxes (not shown), and this helped raise θ_e within the atmospheric column prior to genesis.

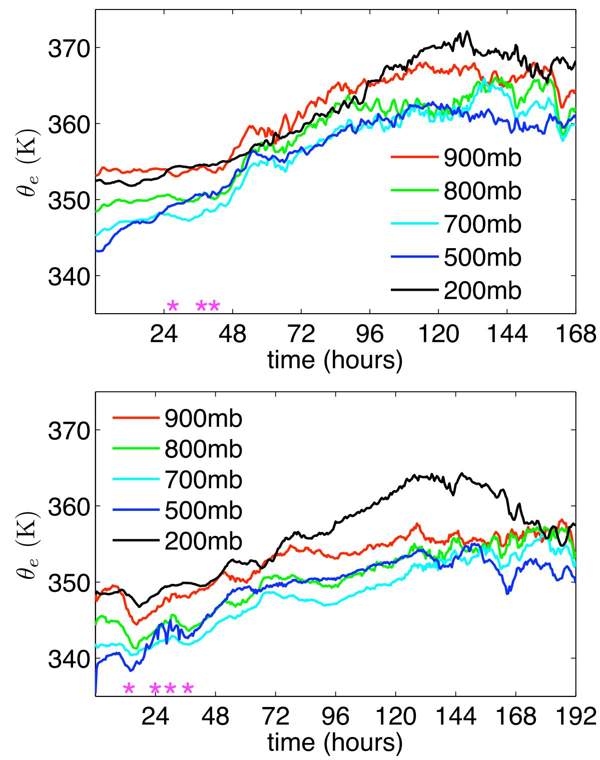

Figure 9: Azimuthally averaged (0-100 km radius) equivalent potential temperature (K) for the Typhoon Ketsana simulation (top) and Typhoon Mawar simulation (bottom). Asterisks denote the time of pre-genesis convective bursts in each simulation.

3.2 Genesis and intensification

By 48 hours, the azimuthally averaged 10 m wind speed had reached tropical storm strength in both simulations, and minimum sea-level pressure had dropped to 988 mb in the Ketsana simulation and 998 mb in the Mawar simulation (Figure 2). Although it is likely that genesis occurred slightly before 48 hours in both simulations, this time, nevertheless, appears significant in the evolution of both systems.

By 48 hours, the azimuthal average of relative humidity had increased significantly from the surface to 500 mb (not shown), approaching 90% up through 500 mb and exceeding 90% closer to the surface. The increase in relative humidity through such a deep layer helped to increase the efficiency by which latent heat could be transferred into the middle and upper-troposphere. Additionally, by 48 hours the near-surface negative temperature anomalies had dissipated in each simulation, and this coupled with the increase in relative humidity allowed for a more rapid development of the warm core in each simulation (not shown).

Both simulations exhibited significant dynamical changes by 48 hours as well. The radius of maximum wind (RMW) shown in Figure 10, which was calculated based on the azimuthally averaged wind speed, reveals that both Ketsana and Mawar experienced a rapid contraction of their wind field leading up to 48 hours. The drop of the RMW through the lower and mid-troposphere increased the inner-core inertial stability. In addition, the rise in moisture by this time coupled with the contraction and "spin-up" of the wind field caused a decrease in the deformation radius. A smaller deformation radius allows the wind field to adjust to the middle and upper-level warming over a spatial scale of similar extent to that of the disturbance, invoking a rotational response that will act to "spin-up" the disturbance. A rapid reduction of the deformation radius was observed in both model simulations prior to genesis (not shown), and is thought to have been a significant step towards genesis.

The rapid contraction of the RMW prior to 48 hours in both simulations suggests that this time marks an important transformation period. Increased inertial stability allowed convective processes embedded within the storm to warm the middle and upper-troposphere more effectively, and a reduction in the deformation radius lead to a local response of the wind field as it adjusted to perturbations in the height field. Both of these processes increased the efficiency by which each of the simulated vortices intensified.

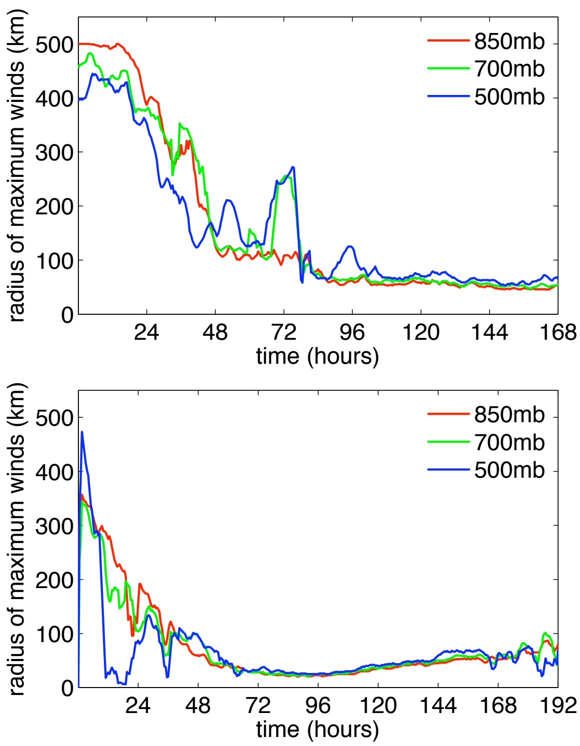

Figure 10: Radius of maximum winds (km) based on the azimuthally averaged wind speed for the Typhoon Ketsana simulation (top) and Typhoon Mawar simulation (bottom). The data were smoothed using a 2.5-hour running mean.

4. CONCLUSIONS

The processes prior to and during tropical cyclogenesis were studied by modeling two real-life tropical cyclogenesis events using the WRF-ARW numerical model. Although Ketsana (2003) and Mawar (2005) differed substantially in both size and structure as mature storms, the model simulations suggest they shared a similar development process through tropical cyclogenesis.

Both simulations exhibited bursts of deep convection prior to genesis. The pre-genesis convective bursts appear to have played a vital role in the development of each storm. Deep convection helped transport high-θ_e air from the boundary layer into the middle and upper-troposphere; this in combination with enhanced surface heat fluxes allowed for an increase in θ_e within the atmospheric column. Evaporative cooling within the boundary layer during the convective bursts led to the development of a near-surface cold pool that helped sustain convection through the forced ascent of converging low-level high-θ_e air.

Positive midlevel PV anomalies formed in each simulation as a result of the convective bursts, and seem to have been enhanced through stratiform processes. Although relative vorticity appears to have increased from the "bottom-up" in the Ketsana simulation, an analysis of the relative vorticity anomaly reveals that midlevel relative vorticity was increasing at the same time as low-level relative vorticity. Although it is not entirely clear what role the midlevel PV anomalies had in the development of each storm, the fact that convection occurred in bursts prior to genesis rather than exhibiting a steady increase in intensity suggests stratiform processes were important. It is hypothesized that increased midlevel relative vorticity associated with the midlevel PV anomalies helped drive the low-level convergence that allowed lower-tropospheric convective processes to "spin-up" Ketsana and Mawar through the convergence of relative vorticity.

Both modeled storms experienced tropical cyclogenesis near 48 hours when significant changes in their thermodynamic and dynamic structure were noted. By 48 hours, the cold pool had dissipated in both simulations, and an increase in moisture was evident through the middle and lower-troposphere, helping to raise the efficiency by which latent heat was transferred into the mid-troposphere. A rapid contraction of the radius of maximum winds prior to genesis raised the inertial stability, and this coupled with the increase in moisture reduced the deformation radius. The increase in inertial stability enhanced warm core development in each of the modeled storms and the reduction of the deformation radius allowed the wind field to "spin-up" and adjust to the midlevel temperature perturbation over a spatial scale similar to that of each disturbance.

Acknowledgements:

We thank the National Center for Environmental Prediction (NCEP) for providing the meteorological data and the National Center for Atmospheric Research (NCAR) for developing and providing support for the Advanced Weather Research and Forecasting (WRF-ARW) model. This research project was made possible in part by a Science Foundation Arizona graduate research fellowship. The research was also supported in part by the Office of Naval Research Marine Meteorology Program under grant #N00014-07-1-0185.

References:

Bister, M. and K. A. Emanuel, 1997: The genesis of Hurricane Guillermo: TEXMEX analyses and a modeling study. *Mon. Wea. Rev.*, **125**, 2662–2682.

Chen, S. S. and W. M. Frank, 1993: A numerical study of the genesis of extratropical convective mesovortices. Part I: Evolution and dynamics. *J. Atmos. Sci.*, **50**, 2401–2426.

Davis, C. A. and T. J. Galarneau Jr., 2009: The vertical structure of mesoscale convective vorticies. *J. Atmos. Sci.*, **66**, 686–704.

Fritsch, J. M., J. D. Murphy, and J. S. Kain, 1994: Warm core vortex amplification over land. *J. Atmos. Sci.*, **51**, 1780–1807.

Hendricks, E. A., M. T. Montgomery, and C. A. Davis, 2004: The role of vortical hot towers in the formation of Tropical Cyclone Diana (1984). *J. Atmos. Sci.*, **61**, 1209–1232.

JTWC, 2003: 2003 annual tropical cyclone report. Tech. rep., U.S. Naval Pacific Meteorology and Oceanography Center / Joint Typhoon Warning Center, 827 pp., [Available from http://metocph.nmci.navy.mil/jtwc/atcr/2003atcr/2003atcr.pdf]

JTWC, 2005: 2005 annual tropical cyclone report. Tech. rep., U.S. Naval Maritime Forecast Center / Joint Typhoon Warning Center, [Available from http://metocph.nmci.navy.mil/jtwc/atcr/2005atcr/].

Montgomery, M. T., M. E. Nicholls, T. A. Cram, and A. B. Saunders, 2006: A vortical hot tower route to tropical cyclogenesis. *J. Atmos. Sci.*, **63**, 355–386.

Ritchie, E. A. and G. J. Holland, 1997: Scale interactions during the formation of Typhoon Irving. *Mon. Wea. Rev.*, **125**, 1377–1396.

Schubert, W. H. and J. J. Hack, 1982: Inertial stability and tropical cyclone development. *J. Atmos. Sci.*, **39**, 1687–1697.

Tory, K. J., N. E. Davidson, and M. T. Montgomery, 2007: Prediction and diagnosis of tropical cyclone formation in an NWP system. Part III: Diagnosis of developing and nondeveloping storms. *J. Atmos. Sci.*, **64**, 3195–3213.

Tory, K. J., M. T. Montgomery, and N. E. Davidson, 2006a: Prediction and diagnosis of tropical cyclone formation in an NWP system. Part I: The critical role of vortex enhancement in deep convection. *J. Atmos. Sci.*, **63**, 3077–3090.

Tory, K. J., M. T. Montgomery, N. E. Davidson, and J. D. Kepert, 2006b: Prediction and diagnosis of tropical cyclone formation in an NWP system. Part II: A diagnosis of Tropical Cyclone Chris formation. *J. Atmos. Sci.*, **63**, 3091–3113.

Zehr, R. M., 1992: Tropical cyclogenesis in the western north Pacific. NOAA Technical Report NESDIS 61, U. S. Department of Commerce, 181 pp. 755